

Electronic Supplementary Information for:

A high-performance photovoltaic small molecule developed by modifying the chemical structure and optimizing the morphology of active layer

Wang Ni,§ Miaomiao Li,§ Xiangjian Wan\*, Huanran Feng, Bin Kan, Yi Zuo, Yongsheng Chen\*

*Key Laboratory of Functional Polymer Materials, Collaborative Innovation Center of Chemical Science and Engineering (Tianjin), Center for Nanoscale Science and Technology, Institute of Polymer Chemistry, College of Chemistry, Nankai University, Tianjin 300071, China.*

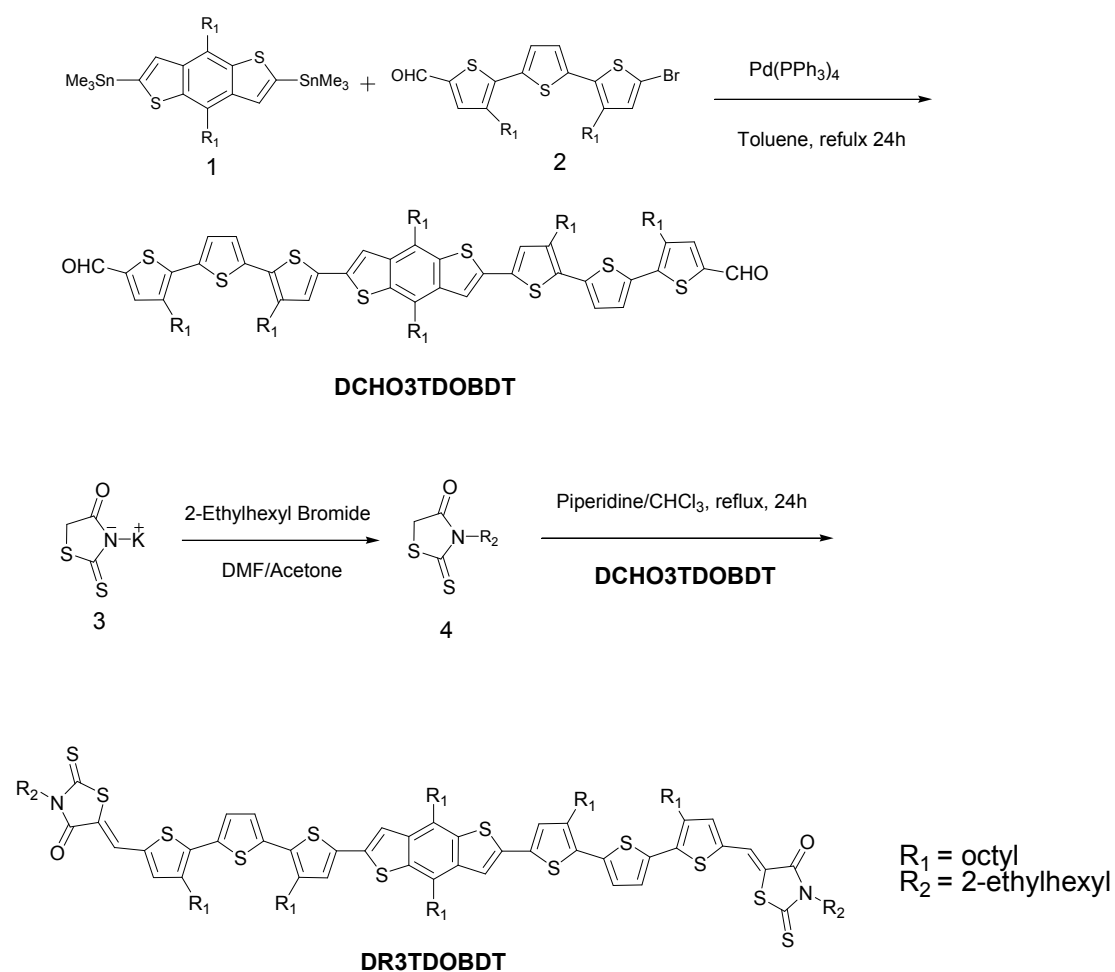
*Email dress:yschen99@nankai.edu.cn;xjwan@nankai.edu.cn*

§ The first two authors contributed equally to this work

**Materials:** All reactions and manipulations were carried out under argon atmosphere with the use of standard Schlenk tube techniques. All starting materials were used as purchased from commercial sources unless stated otherwise. Toluene was distilled from sodium and benzophenone under an Ar atmosphere.  $\text{CHCl}_3$  was dried over anhydrous  $\text{Na}_2\text{SO}_4$ .

## Synthesis

2,6-Bis(trimethyltin)-4,8-dioctylbenzo[1,2-b:4,5-b']dithiophene (**1**), 5-bromo-3,3-dioctyl-2,2':5,2''-terthiophene-2-carbaldehyde (**2**), potassium 4-oxo-2-thioxothiazolidin-3-ide (**3**) and 3-(2-ethylhexyl)-rhodanine (**4**) were prepared according to the literature.<sup>1</sup>



**Scheme S1** Synthesis route of DR3TDOBDT.

### Synthesis of 3-(2-ethylhexyl)-rhodanine (**4**)

2-Ethylhexyl Bromide (9.0 g, 46.6 mmol) was slowly added to a suspension of **3** (1.75 g, 10.2 mmol) and KI (5.08 g, 30.6 mmol) in

acetone (30 ml) and DMF (30 ml). After stirring at 90 °C for 24 h, the reaction mixture was poured into water (200 mL) and extracted with CHCl<sub>3</sub>. The organic layer was washed with water, and then dried over Na<sub>2</sub>SO<sub>4</sub>, and evaporated. The residue was purified by column chromatography on silica gel using a mixture of petroleum and dichloromethane ether (1:2) as eluent to afford 3-(2-ethylhexyl)-rhodanine (1.50 g, 60 %) as a yellow oil liquid. <sup>1</sup>H NMR (400 MHz, CDCl<sub>3</sub>): δ 3.94 (s, 2H), 3.81 (d, *J* = 7.6 Hz, 2H), 1.90 (m, 1H), 1.21 (m, 8H), 0.82 (t, *J* = 7.2 Hz). <sup>13</sup>C NMR (100 MHz, CDCl<sub>3</sub>): δ 201.69, 174.25, 48.47, 36.63, 35.37, 30.38, 28.33, 23.80, 22.96, 14.05, 10.48.

### **Synthesis of DCHO3TDOBDT**

A solution of **1** (1.9 g, 3.28 mmol) and **2** (1 g, 1.35 mmol) in dry toluene (40 mL) was degassed twice with argon followed by the addition of Pd(PPh<sub>3</sub>)<sub>4</sub> (30 mg, 0.026 mmol). After stirring at 100 °C for 24 h under argon, the mixture was poured into water (200mL), and extracted with CHCl<sub>3</sub>. The organic layer was washed with water, and then dried over Na<sub>2</sub>SO<sub>4</sub>, and evaporated. The residue was purified by silica gel chromatography using a mixture of petroleum and dichloromethane ether (1:2) as eluant to afford compound DCHO3TDOBDT (1.4 g, 73%). <sup>1</sup>H NMR (400 MHz, CDCl<sub>3</sub>): δ 9.83 (s, 2H), 7.60 (s, 2H), 7.45 (s, 2H), 7.26 (d, *J*=4.0Hz, 2H), 7.17 (d, 2H), 7.15 (d, *J*=4.0 Hz, 2H), 3.10 (t, *J*=7.2 Hz, 4H), 2.82 (m, 8H), 1.81 (m, 4H), 1.71 (m, 8H), 1.30 (m, 60H), 0.89 (m,

18H).  $^{13}\text{C}$  NMR(100 MHz,  $\text{CDCl}_3$ ):  $\delta$  182.50, 141.06, 140.98, 140.27, 140.16, 139.09, 137.982, 137.05, 136.85, 136.05, 135.94, 134.60, 129.90, 128.57, 128.05, 127.794, 126.08, 117.75, 33.40, 31.97, 31.92, 31.88, 30.51, 30.29, 30.018, 29.71, 29.53, 29.45, 29.33, 22.71, 14.14. MS (MALDI-TOF): calcd for  $\text{C}_{84}\text{H}_{114}\text{O}_2\text{S}_8[\text{M}^+]$ , 1410.66; found:1410.67.

### **Synthesis of compound DR3TDOBBDT**

DCHO3T(O-BDT) (0.30 g, 0.21 mmol) was dissolved in a solution of dry  $\text{CHCl}_3$  (60 mL), then **4** (0.54 g, 2.1 mmol) were added, three drops of piperidine, and the resulting solution was refluxed and stirred for 12 h under argon. Then, the mixture was poured into water (200mL), and extracted with  $\text{CHCl}_3$ . The organic layer was washed with water, and then dried over  $\text{Na}_2\text{SO}_4$ , and evaporated. The residue was purified by silica gel chromatography using a mixture of petroleum and dichloromethane ether(1:1) as eluant, the crude solid was recrystallized from hexane and  $\text{CHCl}_3$  mixture afford DR3TDOBBDT (0.18 g, 46%).  $^1\text{H}$  NMR (400 MHz,  $\text{CDCl}_3$ ):  $\delta$  7.69 (s, 2H), 7.35 (s, 2H), 7.15-7.19 (m, 4H), 7.08-7.12 (m, 4H), 4.02 (m, 4H), 3.04 (m, 4H), 2.79 (m, 8H), 2.05 (m, 2H), 1.81 (m, 4H), 1.71 (m, 8H), 1.32 (m, 76H), 0.90 (m, 30H).  $^{13}\text{C}$  NMR (100 MHz,  $\text{CDCl}_3$ ): 192.58, 167.92, 140.87, 139.44, 137.62, 137.13, 137.05, 136.86, 135.93, 135.17, 134.67, 130.13, 128.52, 128.01, 127.11, 125.97, 124.67, 120.34, 117.66, 48.69, 37.03, 33.43, 32.00, 31.94, 30.55, 30.47, 30.25, 30.06, 29.85, 29.77, 29.72, 29.63, 29.54, 29.48, 29.32, 28.48, 23.96,

23.00, 22.73, 14.13, 14.06, 10.56. MS (MALDI-TOF): calcd for  $C_{106}H_{148}N_2O_2S_{12} [M^+]$ , 1864.82; found:1864.80. Elemental analysis calcd for  $C_{106}H_{148}N_2O_2S_{12}$ : C, 68.19; H, 7.99; N; 1.50%; found: C, 68.09; H, 8.01; N, 1.64%.

## Measurements and instruments

The  $H^1$  and  $C^{13}$  nuclear magnetic resonance NMR spectra were taken on a Bruker AV400 Spectrometer. Matrix assisted laser desorption/ionization time-of-flight mass spectrometry (MALDI-TOF MS) were performed on a Bruker Autoflex III instrument. The transmission electron microscope (TEM) investigation was performed on a Philips Technical G<sup>2</sup> F20 at 200 kV.. The thermogravimetric analysis (TGA) studies were carried out on a NETZSCH STA 409PC instrument under purified nitrogen gas flow with a 10 °C min<sup>-1</sup> heating rate. UV-Vis spectra were obtained with a JASCO V-570 spectrophotometer. X-ray diffraction (XRD) experiments were performed on a Bruker D8 FOCUS X-ray diffractometer with Cu K $\alpha$  radiation ( $k = 1.5406 \text{ \AA}$ ) at a generator voltage of 40 kV and a current of 40 mA. Atomic force microscope (AFM) investigation was performed using Bruker MultiMode 8 in "tapping" mode. Cyclic voltammetry (CV) experiments were performed with a LK98B II Microcomputer-based Electrochemical Analyzer in dichloromethane solutions. All measurements were carried out at room temperature with a conventional three-electrode configuration employing

a glassy carbon electrode as the working electrode, a saturated calomel electrode (SCE) as the reference electrode, and a Pt wire as the counter electrode. Dichloromethane was distilled from calcium hydride under dry argon immediately prior to use. Tetrabutylammonium phosphorus hexafluoride ( $\text{Bu}_4\text{NPF}_6$ , 0.1 M) in dichloromethane was used as the supporting electrolyte, and the scan rate was  $100 \text{ mV s}^{-1}$ .

The current density-voltage ( $J$ - $V$ ) characteristics of photovoltaic devices were obtained by a Keithley 2400 source-measure unit. The photocurrent was measured under illumination simulated  $100 \text{ mW cm}^{-2}$  AM1.5G irradiation using a xenon-lamp-based solar simulator [Oriel 96000 (AM1.5G)] in an argon filled glove box. Simulator irradiance was characterized using a calibrated spectrometer and illumination intensity was set using a certified silicon diode. External quantum efficiency (EQE) value of the encapsulated device was obtained with a halogen-tungsten lamp, monochromator, optical chopper, and lock-in amplifier in air and photon flux was determined by a calibrated silicon photodiode.

SCLC mobility was measured using a diode configuration of ITO/PEDOT:PSS/donor:PC<sub>71</sub>BM/Au by taking the dark current density in the range of 0-7 V and fitting the results to a space charge limited form, where SCLC is described by:

$$\ln \frac{JL^3}{V^2} = \ln\left(\frac{9}{8} \varepsilon_r \varepsilon_0 \mu_0\right) + 0.89\beta \sqrt{\frac{V}{L}} = k \sqrt{\frac{V}{L}} + C$$

$$k = 0.89\beta; C = \ln\left(\frac{9}{8} \varepsilon_r \varepsilon_0 \mu_0\right)$$

where  $J$  is the current density,  $L$  is the film thickness of the active layer,  $\mu_h$  is the hole mobility,  $\epsilon_r$  is the relative dielectric constant of the transport medium,  $\epsilon_0$  is the permittivity of free space ( $8.85 \times 10^{-12}$  F m<sup>-1</sup>),  $V$  ( $= V_{\text{appl}} - V_{\text{bi}}$ ) is the internal voltage in the device, where  $V_{\text{appl}}$  is the applied voltage to the device and  $V_{\text{bi}}$  is the built-in voltage due to the relative work function difference of the two electrodes.

### **Fabrication of organic solar cells**

The photovoltaic devices were fabricated with a structure of glass/ITO/PEDOT:PSS/donor:acceptor/ZnO/Al. The ITO-coated glass substrates were cleaned by ultrasonic treatment in detergent, deionized water, acetone, and isopropyl alcohol under ultrasonication for 15 minutes each time and subsequently dried by a nitrogen flow. A thin layer of PEDOT:PSS (Baytron P VP AI 4083, filtered at 0.45  $\mu\text{m}$ ) was spin-coated (3000 rpm, ca. 40 nm thick) onto ITO surface. After being baked at 150 °C for 20 min, the substrates were transferred into an argon-filled glove box. The active layer was then spin-casted from a blend (w:w) of donor materials and PC<sub>71</sub>BM in different ratios in a chloroform solution at 1700 rpm for 20 seconds on the ITO/PEDOT:PSS substrate. Then, the blend films of active layer were processed with different treatment (without post process, with TA process and with TSA process). Subsequently, ZnO particles solution<sup>2</sup> was spin-casted on top of active

layers. Finally, a 50 nm Al layer were deposited in sequence on ZnO film under high vacuum ( $< 2 \times 10^{-4}$  Pa). The thickness of ZnO and the active layer was measured using Dektak 150 profilometer. The effective area of cells were 4 mm<sup>2</sup> and 12 mm<sup>2</sup> defined by different masks for the solar cell devices discussed in this work. Most photovoltaic performance of devices was tested based on active area of 4 mm<sup>2</sup> unless specially stated.

**Table S1** Optical and electrochemical data of DR3TDOBDT

| Compound  | $\lambda_{\max}$<br>solution<br>/nm | $\epsilon$<br>solution<br>/M <sup>-1</sup> cm <sup>-1</sup> | $\lambda_{\max}$<br>film/<br>nm | $\epsilon$<br>film/<br>cm <sup>-1</sup> | $E_g^{\text{opt}}$<br>eV | $E_g^{\text{CV}}$<br>eV | HOMO/<br>eV | LUMO/<br>eV |
|-----------|-------------------------------------|-------------------------------------------------------------|---------------------------------|-----------------------------------------|--------------------------|-------------------------|-------------|-------------|
| DR3TDOBDT | 511                                 | $8.4 \times 10$                                             | 583                             | 6.5                                     | 1.79                     | 1.81                    | -5.08       | -3.27       |

**Table S2** Photovoltaic performance of BHJ solar cells based on DR3TDOBDT:PC<sub>71</sub>BM with weight ratios (w:w) of 1:0.5, 1:0.8 and 1:1 cast from CHCl<sub>3</sub> followed by TSA treatment and using ZnO/Al as the cathode under an illumination of AM 1.5 G, 100 mW cm<sup>-2</sup>.

| Ratio | $V_{oc}/V$ | $J_{sc}/\text{mA cm}^{-2}$ | FF   | PCE (%) |
|-------|------------|----------------------------|------|---------|
| 1:0.5 | 0.93       | 11.12                      | 0.69 | 7.13    |
| 1:0.8 | 0.94       | 12.56                      | 0.70 | 8.26    |
| 1:1   | 0.93       | 11.90                      | 0.70 | 7.74    |

**Table S3** Photovoltaic performance of BHJ solar cells based on DR3TDOBDT:PC<sub>71</sub>BM (w:w, 1:0.8) with thickness of 80 nm, 120 nm, 150 nm cast from CHCl<sub>3</sub> followed by TSA treatment and using ZnO/Al as the cathode under illumination of AM 1.5 G, 100 mW cm<sup>-2</sup>.

| Thickness of the<br>active layer (nm) | $V_{oc}/V$ | $J_{sc}/\text{mA cm}^{-2}$ | FF   | PCE (%) |
|---------------------------------------|------------|----------------------------|------|---------|
| 80                                    | 0.94       | 11.17                      | 0.69 | 7.24    |
| 120                                   | 0.94       | 12.56                      | 0.70 | 8.26    |

|     |      |       |      |      |
|-----|------|-------|------|------|
| 150 | 0.94 | 11.82 | 0.68 | 7.55 |
|-----|------|-------|------|------|

**Table S4** Current density-voltage characteristics of the bulk BHJ solar cells based on DR3TDOBDT: PC<sub>71</sub>BM (1:0.8, w/w) blend films with different post- treatments.

| Process methods of the photoactive layer | V <sub>oc</sub> /V | J <sub>sc</sub> /mA cm <sup>-2</sup> | FF (%) | PCE (%)           |
|------------------------------------------|--------------------|--------------------------------------|--------|-------------------|
| Without post treatment                   | 0.98               | 8.52                                 | 52.0   | 4.34 <sup>a</sup> |
| Without post treatment                   | 0.98               | 8.40                                 | 51.0   | 4.20 <sup>b</sup> |
| Thermal annealing                        | 0.96               | 11.34                                | 60.0   | 6.53 <sup>a</sup> |
| Thermal annealing                        | 0.96               | 11.14                                | 58.7   | 6.28 <sup>b</sup> |
| TSA treatment                            | 0.94               | 12.56                                | 70.0   | 8.26 <sup>a</sup> |
| TSA treatment                            | 0.94               | 12.30                                | 68.4   | 7.91 <sup>b</sup> |

a The active area is 0.04 cm<sup>2</sup>; b The active area is 0.12 cm<sup>2</sup>

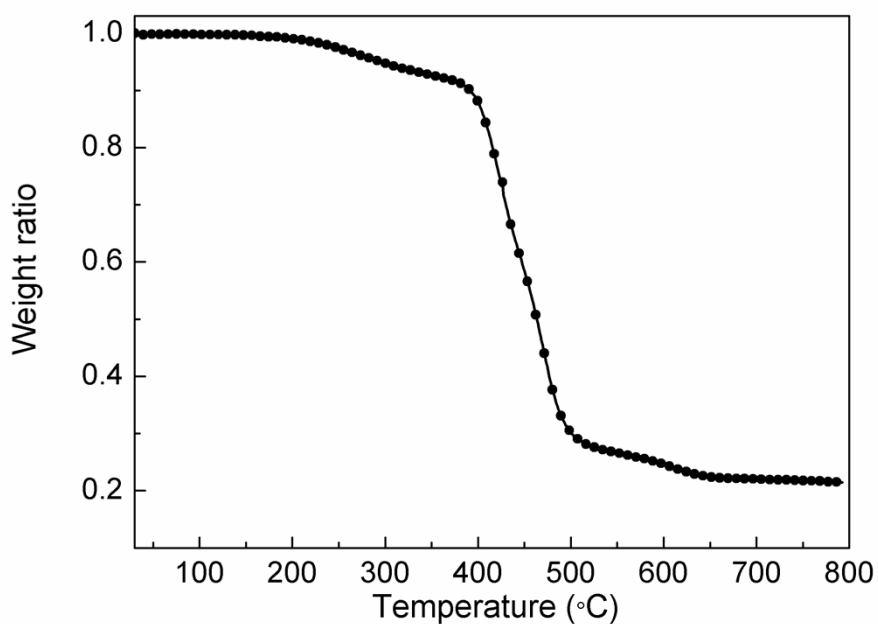


**Fig. S1.** TGA curve of DR3TDOBDT with a heating rate of 10 °C/min under N<sub>2</sub> atmosphere.

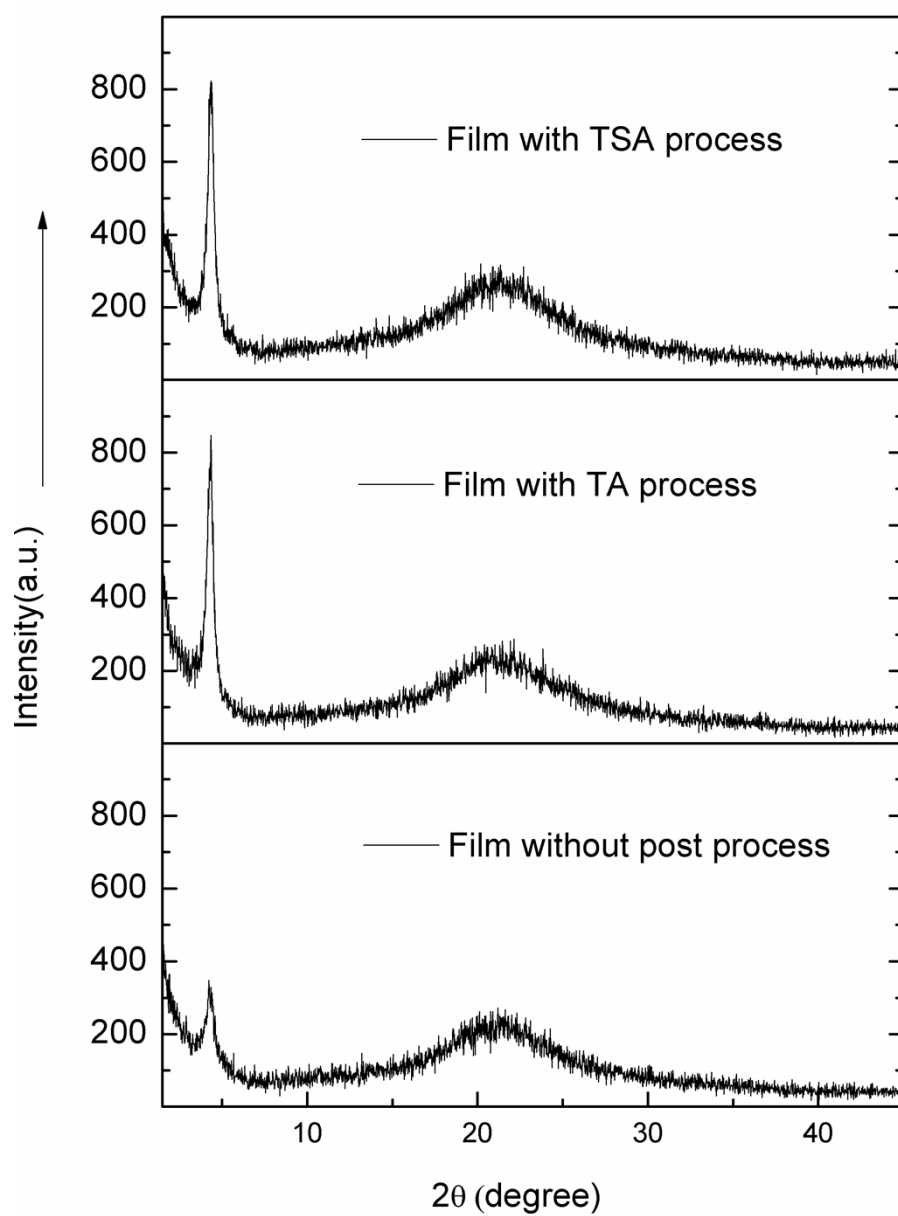


**Fig. S2.** XRD patterns of DR3TDOBDT:PC<sub>71</sub>BM blend films spin-coated from CHCl<sub>3</sub> onto glass substrate with different post treatment.

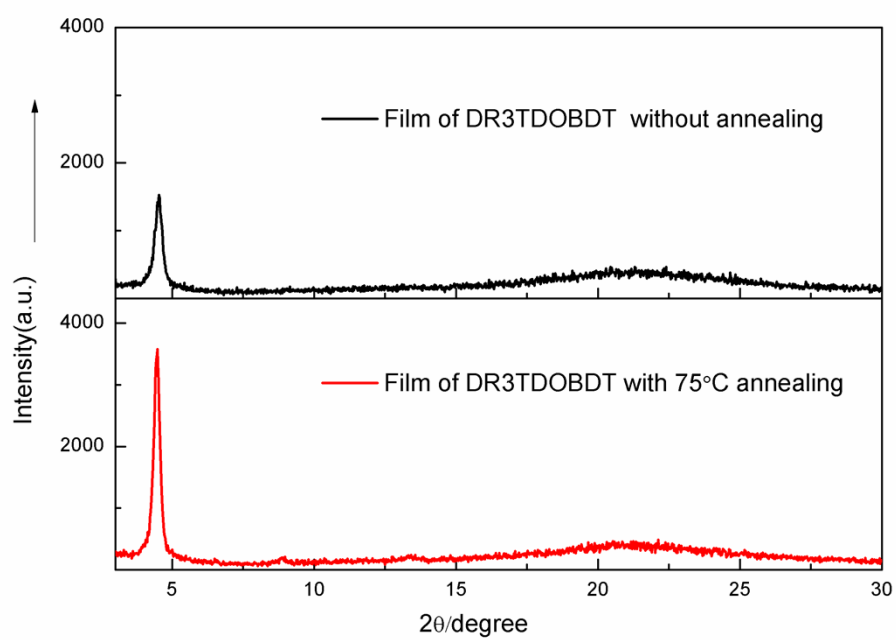


**Fig. S3.** XRD patterns of DR3TDOBDT films spin-coated from  $\text{CHCl}_3$  onto glass substrate.

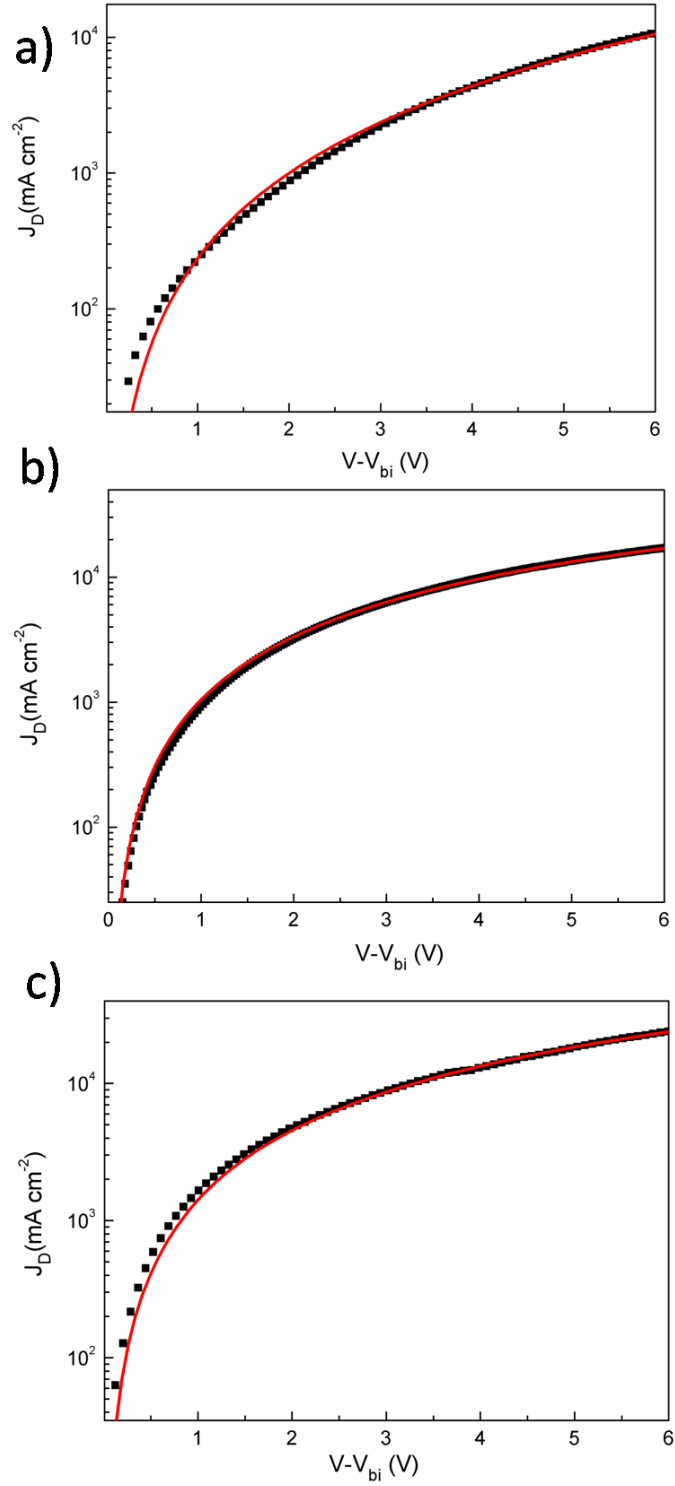


**Fig. S4.**  $J$ - $V$  characteristics of a hole-only device with the configuration ITO/PEDOT:PSS (30 nm)/DR3TDOBDT:PC<sub>71</sub>BM without ETL/Au (30 nm). (a) device without post treatment, (b) device with TA treatment, c) device with TSA treatment. The solid lines represent the fit using a model of single carrier SCLC with field-independent mobility. The  $J_D$ - $V$  characteristics are corrected for the built-in voltage  $V_{bi}$  that arises from the work function difference between the contacts.

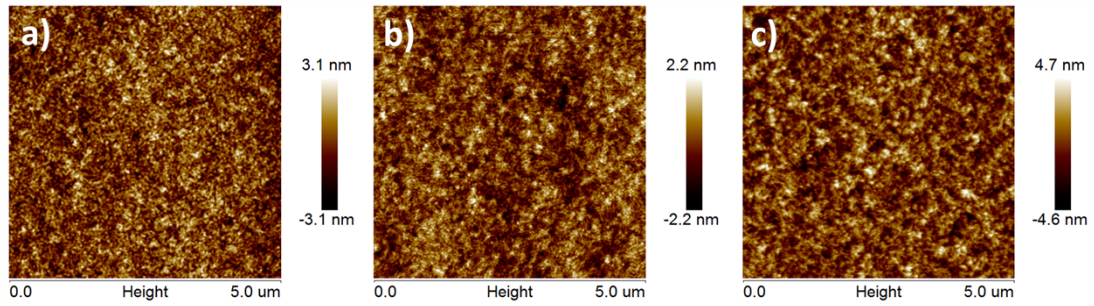


**Fig. S5.** Tapping-mode AFM height images of the active layers with DR3TDOBDT/PC<sub>71</sub>BM (1:0.8,w/w) (a) no post treatment, (b) with TA treatment, c) with TSA treatment.

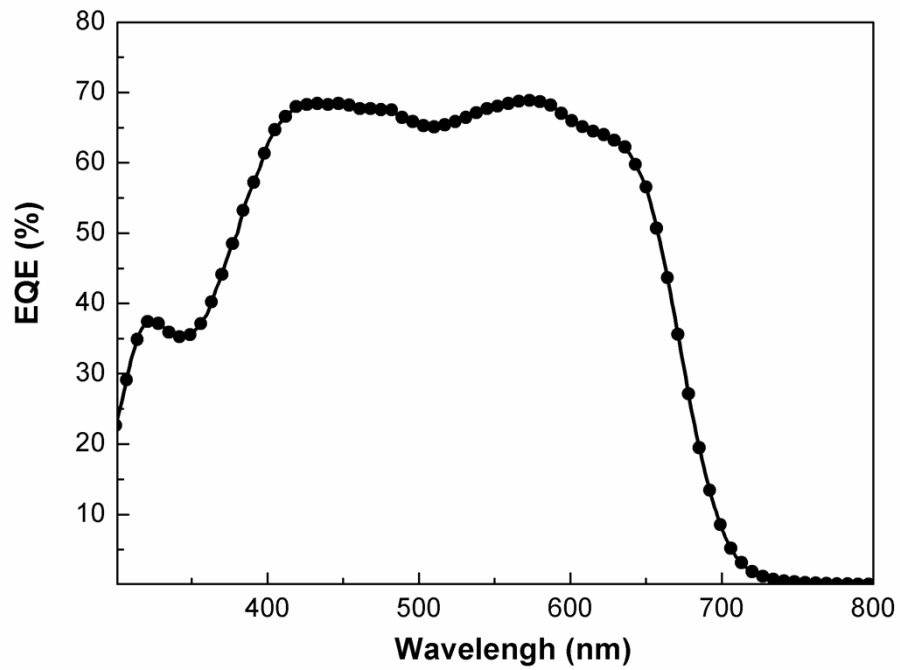


**Fig. S6** EQE of device based on DR3TDOBDT:PC<sub>71</sub>BM (1:0.8, w/w) blend film with TSA treatment.

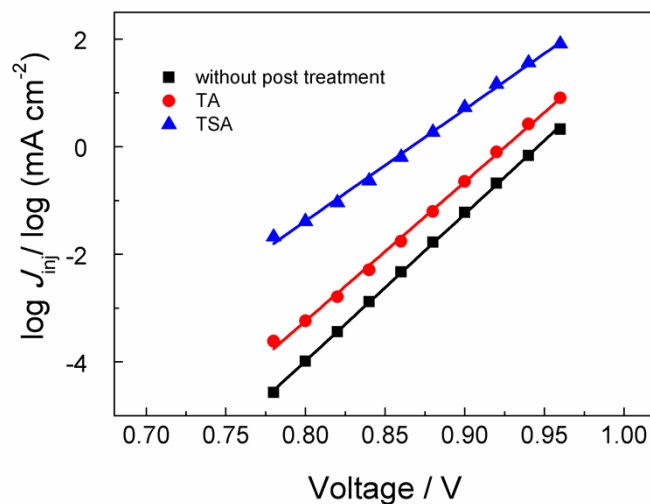


**Fig. S7** The fitted dark injected current  $J_{inj}$  versus voltage  $V$  for DR3TDOBDT:PC<sub>71</sub>BM (1:0.8, w/w) blend films with different treatment<sup>a</sup>.

<sup>a</sup> The dark injected current  $J_{inj}$  versus applied voltage for donor:fullerene devices was exponentially fitted according to Equation 1, therefore to determine reverse saturation current density  $J_{0,n}$ .

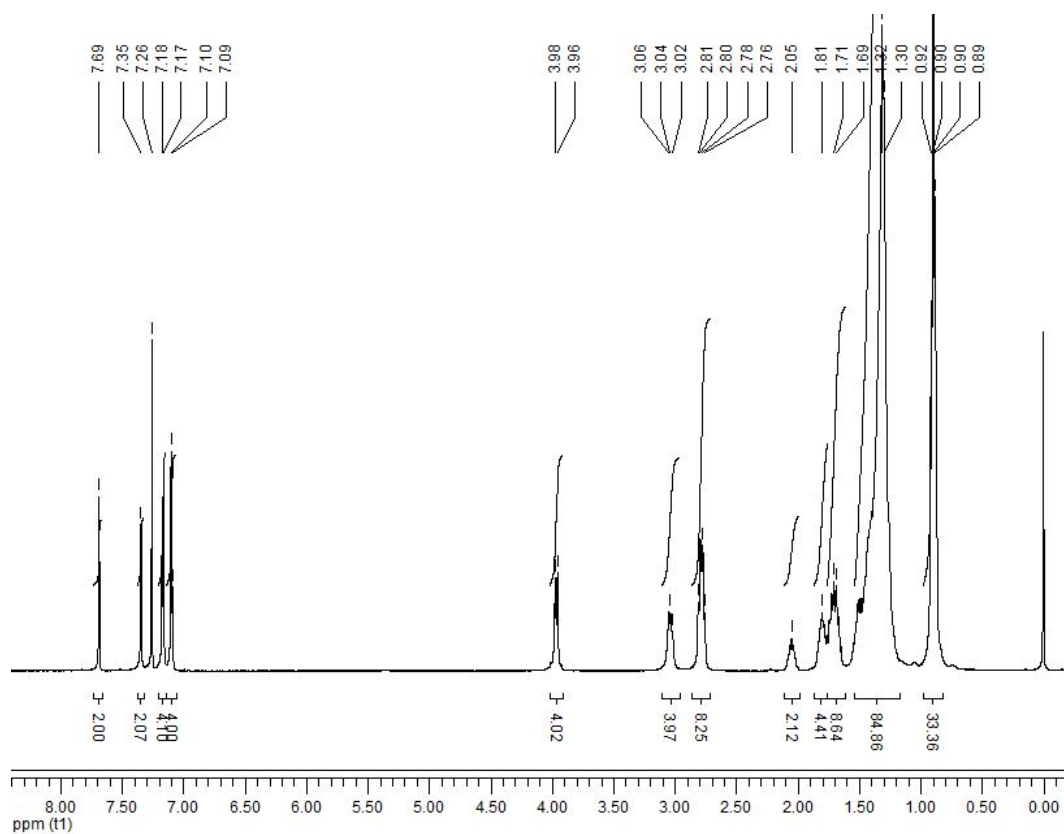
$$J_{inj} = J_{0,n} \exp\left(\frac{qV}{nkT}\right) \quad \text{Equation 1}^3$$

Table S5 Measured and simulated performance parameters for DR3TDOBDT:PC<sub>71</sub>BM (1:0.8, w/w) blend films with different treatment<sup>a</sup>.

| Process methods of the photoactive layer | $V_{oc}/V$ | $J_{0,n}/ \text{mA cm}^{-2}$ | $J_{so}/ \text{mA cm}^{-2}$ |
|------------------------------------------|------------|------------------------------|-----------------------------|
| Without post treatment                   | 0.98       | $6.00 \times 10^{-12}$       | $3.10 \times 10^{-3}$       |
| Thermal annealing                        | 0.96       | $4.17 \times 10^{-11}$       | $8.21 \times 10^{-3}$       |
| TSA treatment                            | 0.94       | $1.54 \times 10^{-8}$        | $1.11 \times 10^{-1}$       |

<sup>a</sup>  $J_{so}$  is calculated according to Equation 2.

$$J_{0,n} = J_{so} \exp\left(\frac{-\Delta E_{DA}}{2nkT}\right) \quad \text{Equation 2}^4$$



**Fig. S8**  $^1\text{H}$  NMR spectra of compound **DR3TDOBDT** at 300K in  $\text{CDCl}_3$ .

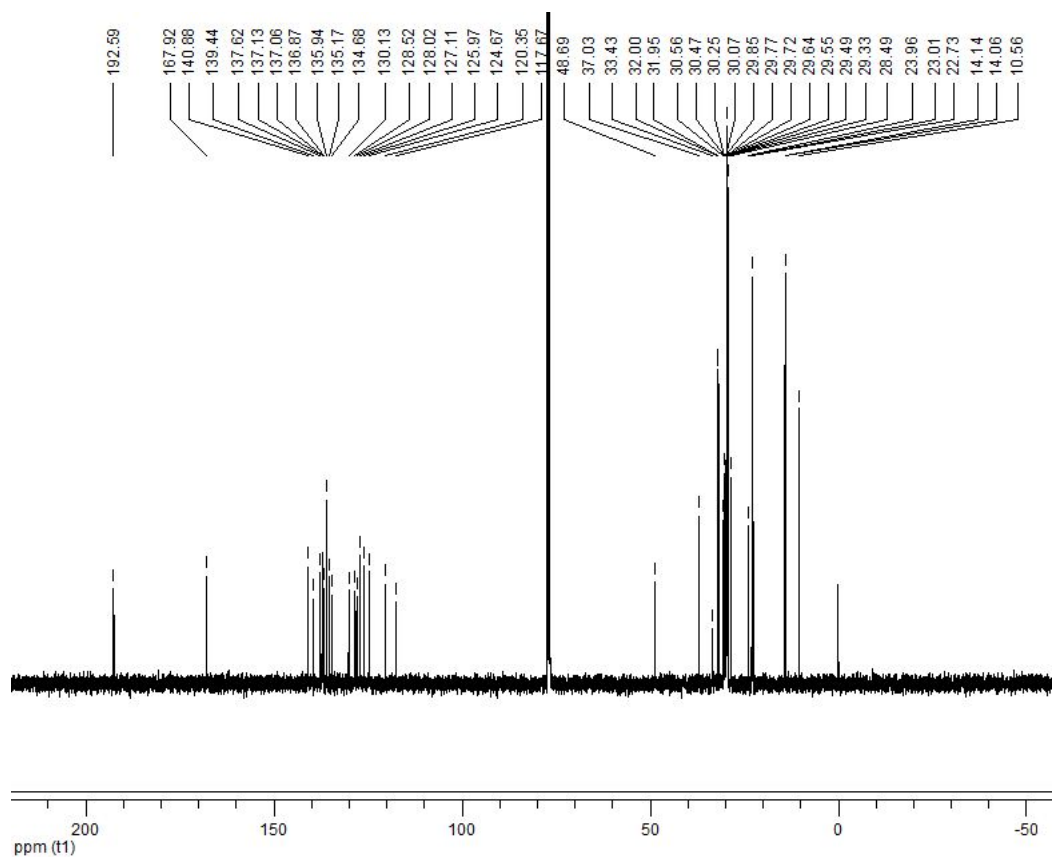


**Fig. S9**  $^{13}\text{C}$  NMR spectra of compound **DR3TDOBDT** at 300K in  $\text{CDCl}_3$ .

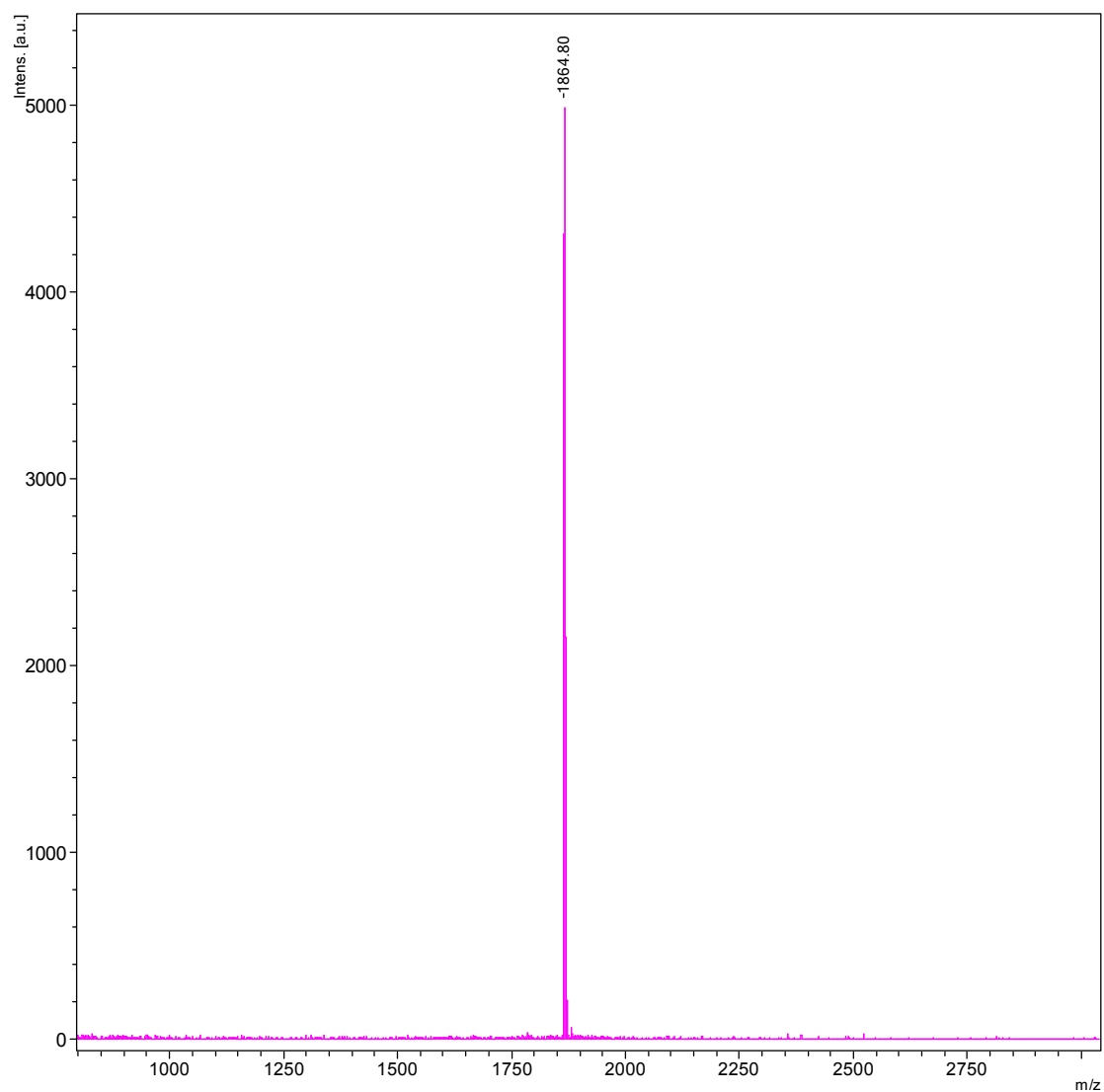


**Fig. S10** The MALDI-TOF plot of compound DR3TDOBBDT.

### Reference

- 1 (a) Y. Liang, D. Feng, Y. Wu, S.-T. Tsai, G. Li, C. Ray and L. Yu, *Journal of the American Chemical Society*, 2009, **131**, 7792; (b) J. Zhou, X. Wan, Y. Liu, G. Long, F. Wang, Z. Li, Y. Zuo, C. Li and Y. Chen, *Chemistry of Materials*, 2011, **23**, 4666; (c) Y. Liu, C.-C. Chen, Z. Hong, J. Gao, Y. Yang, H. Zhou, L. Dou and G. Li, *Sci. Rep.*, 2013, **3**.
- 2 W. J. E. Beek, M. M. Wienk, M. Kemerink, X. Yang and R. A. J. Janssen, *The Journal of Physical Chemistry B*, 2005, **109**, 9505.
- 3 K. Vandewal, K. Tvingstedt, A. Gadisa, O. Inganäs and J. V. Manca, *Nat Mater*, 2009, **8**, 904.
- 4 C. W. Schlenker and M. E. Thompson, *Chemical Communications*, 2011, **47**, 3702.